J. Mat. NanoSci. 2019, 6(2), 38-46 Review

Journal of
Materials NanoScience

# Photodiodes: Principles and recent advances

**Rita F. Pires,* Vasco D. B. Bonifácio***

*CQFM-IN and IBB-Institute for Bioengineering and Biosciences, Instituto Superior Técnico, Universidade de Lisboa, Lisboa, Portugal.*

Submitted on: 19-Mar-2019, Accepted on: 6-July-2019, Published on: 11-July-2019

**ABSTRACT**

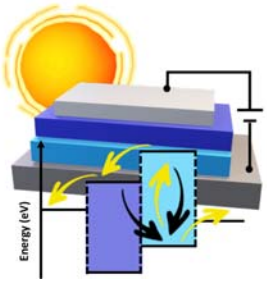


Photodiodes are on the rise. In the past decade many efforts have been made to deliver cheaper, more flexible, and increasingly better performing photodiode devices. The demand for enhanced optoelectronics led to the development of new inorganic, organic, and hybrid materials. In this review we describe in detail the working principles, the characterization, fabrication (types and architectures) and major applications of photodiodes. Recent applications, mainly in imaging, sensing and healthcare are also presented.

*Keywords: Photodiodes, p-n junction, inorganic photodiodes, organic photodiodes, hybrid photodiodes*

## PHOTODIODES

Photodiodes could be described as semiconductors that are able to convert light into electric current. Also called photodetectors, photosensors or light detectors, they are very sensitive to light, allowing a fast conversion, being used in several applications such as biomedicine or image sensing.

The chase for a small size, low cost, long lifetime, low responsive to temperature, high response and sensitivity to light, low noise and high gain photodiode lead to development of new semiconductors (organic, inorganic or hybrid) to improve these qualities and also try to avoid some problems like low dark current and detectivity.[1]

Photodiodes may be classified in several ways, depending on the type of construction (*p-n*, PIN junction or avalanche), spectral response window width (broadband or panchromatic and narrowband, wavelength selective) or by the type of employed semiconductors (organic, inorganic or hybrid).[2]

In this review we provide a concise compilation of essential information about photodiodes, namely basic working principles, fundamental parameters that should be considered during device construction, different types of operation, fabrication and current applications.

## WORKING PRINCIPLES

All photodiodes operate in the same way. The structure of a photodiode can be a *p-n* junction or a PIN junction. A *p-n* junction is the combination of a *p*-type semiconductor (where holes are the majority charge carriers and free electrons are the minority) and a *n*-type semiconductor (free electrons are the majority charge and holes are the minority charge carries). The region where both *p*- and *n*-type semiconductors are joined is called the *p-n* junction. The

*Corresponding Authors: Vasco D.B. Bonifácio and Rita F. Pires
Address: CQFM-IN and IBB-Institute for Bioengineering and Biosciences, Instituto Superior Técnico, Universidade de Lisboa, Lisboa, Portugal
Tel: +351 218 419 218
Email: vasco.bonifacio@tecnico.ulisboa.pt and ritafpires@tecnico.ulisboa.pt

Cite as: *J. Mat. NanoSci., 2019, 6(2), 38-46.*
*urn:nbn:sciencein.jmns.2019v6.89*

©The ScienceIn ISSN 2394-0867
http://pubs.thesciencein.org/jmns

natural tendency is the migration of electrons to holes to reach an equilibrium. However, in the *p-n* junction interface there is a depletion region that slows down electron transfer. In case of a PIN junction, there is an intrinsic semiconductor between the *p*- and *n*-semiconductors.[3]

Usually, the working principle of photodiodes is similar to solar cells. Both *p-n* junctions or PIN semiconductors can be used, but they operate under reverse bias conditions, this means that the *p*-side is connected to the anode and the *n*-side is connected to the cathode. As can be seen in Figure 1, when a photon strikes the diode, an electron hole pair is created (photoelectric effect). If the absorption occurs in a diffusion length of the depletion region or inside the depletion region, these carriers are swept away from the junction through the built-in field of the depletion region. The electrons move towards the cathode and the holes move toward the anode, producing a photocurrent.[4]

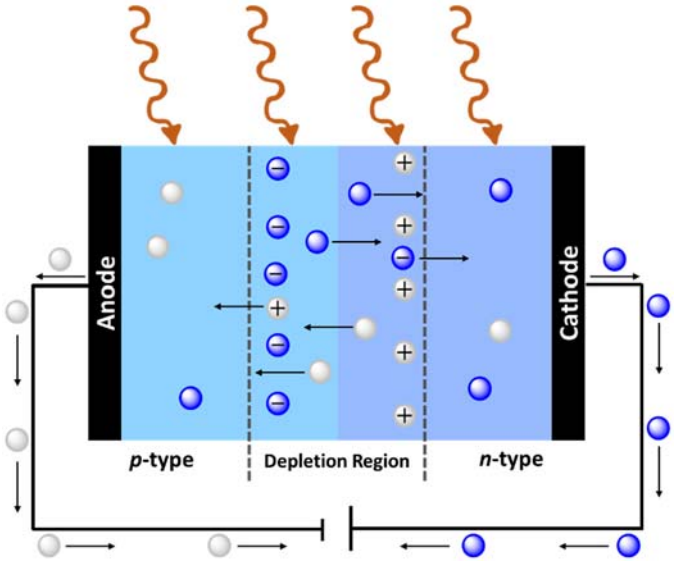


**Figure 1.** Working principle of a *p-n* junction photodiode.

Photodiodes can operate in photovoltaic or photoconductive mode. In the case of a photovoltaic mode, photodiodes work at zero bias. In the case of a photovoltaic mode, photodiodes work at zero bias and the dark current is minimal, thus are suitable for ultralow-light-level applications. Furthermore, the photovoltaic mode offers a simple operational configuration for low-frequency applications. When operating in photoconductive mode, the photodiode is reverse biased. This operation mode is important in case of organic photodiodes since it improves their response speed and linearity in a similar way as that of inorganic silicon semiconductors photodiodes. However, the enhancement of dark current is a drawback.[5]

Different type of photodiodes have been developed to improve specific needs. Besides commom *p-n* and PIN junctions types, previouly described, avalanche photodiodes and Schottky barrier diodes are also an option.

Avalanche photodiodes are basically PIN junctions designed to operate with high reverse bias, approaching the reverse breakdown voltage. This phenomenon is reached when a high electric field is applied and carriers gain kinetic energy, thus generating additional electron-hole pairs through impact ionization. At a certain point the generated photocurrent will increase suddendly, giving origin to an alavalanche breakdown point.[6,7] Mostly build with inorganic materials, these photodiodes are characterized by a detection efficiency, a gain at low bias voltage and a responsivity usually higer as compared to other photodiodes, making them useful, for example as refield valves, protecting the systems from excess voltages, and also in some clinical and biomedical applications (*e.g.* pressure control devices). However, avalanche photodiodes require a very meticulous production, which increases manufacturing costs.[8-10]

Schottky barrier photodiodes are other particular type of photodiodes. Based on a metal-semiconductor (M-S) junction, these photodiodes have high quantum efficiency, speed response, low dark current, high UV-Visible contrast, which are notable advantages of these type of photodiodes. Compared with avalanche photodiodes, they have simliar high response speed but are much easier to fabricate.[11-15]

## PHOTODIODES CHARACTERIZATION

To evaluate the photodiodes performance key parameters must be taken in account, both at an electrical and optical level.[2,5,16,17] An overvierw of this parameters is given below.

**Shunt Resistance ($R_{SH}$)**

Defined as the slope of the current-voltage curve at the origin. Experimentally can be obtained by applying a voltage of ±10 mV, measuring the current and calculating the resistance.

**Series Resistance ($R_S$)**

Used to determine the linearity of the photodiode in the photovoltaic mode, series resistance is a result of the resistance of the contacts and the undepleted material (*e.g.* silicon), and can be calculated using equation 1:

$$R_S = \frac{(W_S - W_d)\rho}{A} + R_C \quad (1)$$

where $W_S$ is the thickeness of the substrate, $W_d$ is the width of the depleted region, A is the diffused area of the junction, ρ is the resistivity of the substrate and $R_C$ is the contact resistance.

**Junction Capacitance ($C_J$)**

Directly proportional to the diffused area and inversely proportional to the width of the depletion region, junction capacitance is obatained using equation 2:

$$C_J = \frac{\epsilon_{Si}\epsilon_0 A}{\sqrt{2\mu\rho(V_A + V_{bi})}} \quad (2)$$

Where $\epsilon_0$ is the permitivity of free space ($8.854 \times 10^{-14}$ $Fcm^{-1}$ for silicon photodiodes), $\epsilon_{Si}$ is the substrate dielectric constant (11.9 in this case), μ (1400 $cm^2Vs^{-1}$) is the mobility of the electrons at 300 K, ρ is the resistivity of the silicon, $V_{bi}$ is the built-in voltage of the substrate and $V_A$ is the applied bias.

**Responsivity (R)**

Responsivity is defined as the ratio between the photocurrent generation and the incident power, that can be calculated using equation 3:

$$R(\lambda) = \frac{I(\lambda)_{ph}}{P(\lambda)_{in}} \quad (3)$$

where $I(\lambda)_{ph}$ is the photocurrent (in amperes) and $P(\lambda)_{in}$ is the incident optical power (in watts).

**External Quantum Efficiency (EQE)**

Defined as the electron number detected per incident photon, EQE is expressed through equation 4:

$$EQE(\lambda) = \frac{R(\lambda)hc}{q\lambda} = \frac{1.24R(\lambda)}{\lambda} \quad (4)$$

where h is the Planck's constant, c is the speed of the light and q is the elementary charge. The operation (hc)/q could be approximated to 1.24 if the λ units are expressed in μm.

**Noise equivalent power (NEP)**

NEP (λ) (expressed in $WHz^{1/2}$) gives the minimum detectable power per square root of bandwidth. It can be calcultated using equation 5:

$$NEP(\lambda) = \frac{\sqrt{\overline{i_n^2}}}{\sqrt{\Delta f}R(\lambda)} \quad (5)$$

where the noise current spectral density is given by $I_n$ and Δf is the electrical bandwidth of the noise measurement. The total noise current is the sum of all noise sources, including the shot noise from dark current and the low-frequency flicker noise (1/f). Also, the root-mean-square (rms) value for shot noise current ($I_{sh}$) is given by $I_{sh} = \sqrt{2q\Delta f I_d}$ , where $I_d$ is the dark current. When the dark current shot noise is dominant, NEP(λ) can be determined using equation 6:

$$NEP(\lambda) = \frac{\sqrt{2qI_d}}{R(\lambda)} \quad (6)$$

**Specific Detectivity (D*)**

Specific detectivity (expressed in $cmHz^{1/2}W^{-1}$) is one of the most important physical parameters, being the figure of merit to describe the ability to detect weak light. It can be calculated using equation 7:

$$D^*(\lambda) = \frac{\sqrt{A}}{NEP(\lambda)} = \frac{R(\lambda)}{\sqrt{2qJ_d}} \quad (7)$$

where A is the device area and $J_d$ is the dark current density. The second deduction can be used assuming that shot noise is the main component of the overall photodiode noise.

**Linear dynamic range (LDR)**

Defined as the range of incident optical powers within which the photocurrent versus power is a linear function. It is expressed in decibels and is calculated using equation 8:

$$LDR(\lambda) = 20log\frac{P(\lambda)_{max}}{P(\lambda)_{min}} = 20log\frac{I(\lambda)_{max}}{I(\lambda)_{min}} \quad (8)$$

where $P(\lambda)_{max}$ is the maximum impinging power above which the response of the device deviates from linearity and $P(\lambda)_{min}$ is the minimum detectable optical power (or noise equivalent power, NEP). This expression can be approximated and use the maximum and the minimum of the photocurrent limit, $I(\lambda)_{max}$ and $I(\lambda)_{min}$, respectively.

**On/off ratio**

This ratio can be calculated as the $I(\lambda)_{ph}$ to $I_d$ ratio at fixed incident optical power and bias voltage conditions, which reflects the photosensitivity of a photodiode.

**3dB bandwidth ($f_{3dB}$)**

Relative to the modulation frequency of input light when *R(λ)* is approximatly 0.707 (1/√2) times higher than the obtained under illumination.

**Frequency response (τ)**

Defined as the frequency response, τ is the time needed for the signal to rise or fall from 10% to 90% (or vice versa) of the final value respectively. This parameter can be estimated using equation 9:

$$\tau = \frac{1}{2\pi f_{3dB}} \quad (9)$$

From all these parameters, EQE and D* are major performance indicators. Figure 2 shows collected data[5,18] for both inorganic, organic and hybrid photodiodes using different architectures, in the period from 1996 to 2018. As can be seen, very good external quantum effiencies and specific detectivities have been already achieved, especialy in the visible region.

The non-uniformity (variations of responsivity at the photodiode active suface area) and non-linearity (variation of the ratio of the change in photocurrent to the same change in light power) are also parameters that should be taken in consideration, as well as the temperature influence in several paramenters, such as the responsivity, in the breakdown voltage and also in the dark current.

Although an "ideal" photodiodes should have the best performance at all levels, until now there is no ideal photodiode yet. Parameters shuch as responsivity, specific detectivity, external quantum efficiency or low dark current can have an huge variety between different devices. Usually the photodiodes developed have one or two excellent parameters performance, but the others are much lower compared to others. For that reason, several devices and materials have been developed and combined to achieve an "ideal performance".

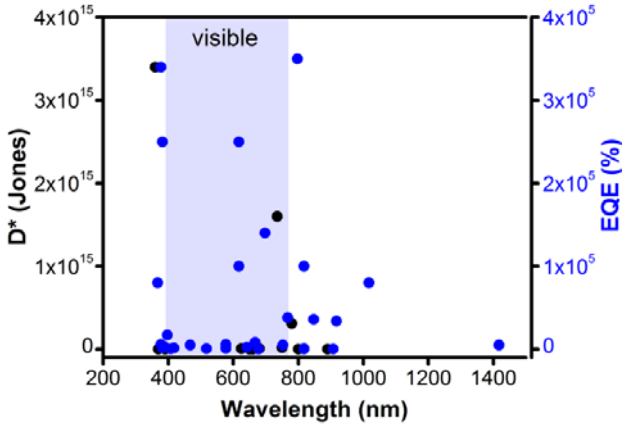


**Figure 2.** External Quantum Effiency (EQE) and Specific Detectivity (D*) of photodiodes reported in the period 1996-2018.

## INORGANIC PHOTODIODES

Currently, most of the commercially availilabe photodiodes are composed by crystalline inorganic semiconductors. Although silicon was the first to be used, several inorganic semiconductors have also been widely used, such as GaP, $Ga_2O_3$, GaAs, AlSb, GaN, InGaAs (III-V semiconductors) or even ZnO, HgCdTe, Ge and CdS, since their high charge carrier mobility, small exciton binding energy, high stability were attractive properties for their extensive study.[2,5,7,19-21]

The purity of the semiconductors and their growth temperature are very important factors that can have a tremendous impact in the photodiodes performance. For example, Arikata *et al.* growth InAs/GaSb superlattice structures in GaSb substrates to be used as IR detectors through a method of metalorganic vapour-phase epitaxy, observing that the growth temperature influenced the results directly and that the highest performance of these devices was only obatined at 20 K (31% EQE at 3.5 µm).[19] Also, El-Amir *et al.* studied the temperature dependence of high purity *n*-type $Mg_2Ge$ single crystals fabricated by thermal annealing, revealing a clear rectifying behaviour and an obvious photoresponse chactracteristic between 0.8 and 1.7 µm, with a maximum zero-biased photoresponse of 7mA$W^{-1}$ at 1.2 µm.[20]

Also, some heterostructure photodiodes such as Sb/$WSe_2$, Ge-on-Si, Cu doped $SnS_2$ nanoflakes, $Bi_2Te_3$-Si, GaSb and GaSb/AlSb superlattice buffer layers grown on Ga or Si have been explored, since combination of different semiconductors improve performance.[22-24] Liu *et al.* combined the unique optoelectronic properties of a topological insulator based photodetector on Si with the complementary metal-oxide-semiconductor (CMOS) technology using for that a Si-based single crystal bismuth telluride ($Bi_2Te_3$) photoconductive detector able to achieve a responsivity of $3.64\times10^{-3}$ $AW^{-1}$ at 1064 nm and $3.32\times10^{-2}$ $AW^{-1}$ at 1550 nm, showing a good potencial for applications in future Si photonics.[24]

Recently, tailorable optical properties (energy band gap and optical constants), large absorption coefficient in the UV–Vis range, long carrier diffusion lengths high charge-carrier mobilities, and low exciton binding energies at room temperature, deploted an huge interest in the development of new 0D, 1D, 2D and 3D type halide perovskites.[25] Colloidal inorganic quantum dots (*e.g.* PbS or Ge) are also on the spot since offer some improvement in solution processability, size tunable spectral sensitivity and higher compatibility with flexible substrates.[26,27]

Tang *et al.* developed a stable, low cost and CMOS compatible Schottky junction photodiode using a Au-PbS colloidal quantum dot-indium tin oxide vertical junction. Under 1550 nm ilumination, the authors achieved not only an EQE of aproximately 400%, but also a responsivity of 5.15 $AW^{-1}$, a D* of $1.96\times10^{10}$ Jones and a response time of 110 µs, fullfilling a statisfatory number of parameters at the same time that can be used in on-chip integrated optoelectronic circuits or infrared focal plane arrays.[26]

Although we have now different available options to work under UV, visible or NIR wavelengths and also some of them work in a broadband spectrum inorganic photodiodes still present major drawbacks. These include expensive and demanding manufacture, mechanical inflexibility, low operating temperatures and high driving voltages, thus narrowing their applications mainly to photodetection.[27]

## ORGANIC PHOTODIODES

Due to their unique properties, organic semiconductors based photodiodes brought a revolution in optoelectronics. An organic semiconductor can be defined as an organic material with semiconducting properties, conferred by π and π* orbital delocalization. There is a huge multiplicity of organic semiconducting materials, covering a large spectrum of optical and spectral properties, that have been fully investigated as working organic photodiodes. These include both small molecules, such as pigments, and conjugated polymers with linear or dendritic architectures. Fullerenes ($C_{60}$, $C_{70}$, $PC_{60}BM$, $PC_{71}BM$) and polymers such as P3HT, F8T2, PEDOT, PSS, PTB7-Th, PPDT2FBT, DPP-DTT, PCPDTBT, PCDTBT, MEH-PPV and P(NDI2OD-T2), are some examples of organic semiconductors that have been widely studied alone or in different cross combinations.[28-33]

Organic semiconductors provide high charge carriers photogeneration yields, tunable optical gaps from UV to NIR, and production of films over large areas (that can be amorphous) using simple and low cost processes (*e.g.* spin-coating, aerosol-jet printing, spray-coating, inject printing or screen printing).[28,29,34] Like in photovoltaic cells, such properties open the possibility of its use in broad applications, beyond photodetection, such as biomedical imaging and sensing, communications, control circuits or machine vision.[35,36]

In organic semiconductors weak van der Walls forces are involved. The electrical properties are not due to electrons and energy bands, like in inorganic semiconductors, but arise from differences in energy levels, the lowest unoccupied molecular original (LUMO) and the highest occupied molecular orbital (HOMO). In Figure 3, a energy-band diagram shows a typical heterojunction organic photodiode and the way it operates.

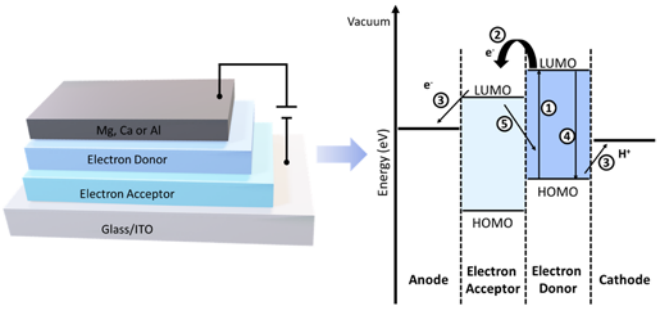


**Figure 3.** Schematic representation of a heterojunction organic photodiode with the representation of the energy band diagram. When both LUMO and HOMO of the donor lie at energies sufficiently higher than those of the acceptor, it will be energetically favorable for an exciton to reach the interface to dissociate, leaving a negative polaron on the acceptor and a positive polaron on the donor. For efficient photocurrent generation the charge separation (2) should be readily followed by a geminate recombination (4) after a photon absorption event (1), and where the transfer to contacts (3) should compete with interfacial recombination (5).[29]

The first and simplest organic photodiode was made by a layer of the organic material sandwiched between a anode, typically indium tin oxide (ITO), and a cathode (usually low work function metals such as Al, Ca, or Mg). However, due to the lack of direct separation of the exciton into free charges, caused by the week screening of the Coulomb interactions of the electron-hole pair, the quantum yield of these homojunctions was very low.

In this sense, planar bilayer heterojunctions (Figure 3) and bulk heterojunctions (BHJ) architectures (Figure 4) came up as a solution for more efficient devices. With an interface between electron donor and acceptor species, electrostatic forces are produced due to differences in electron affinity and ionization potential.

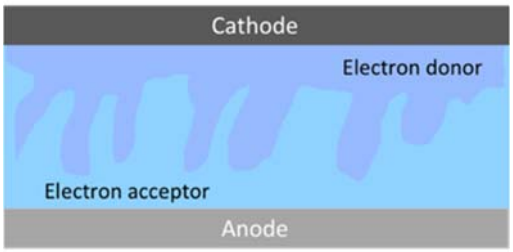


**Figure 4.** Schematic representation of a BHJ organic photodiode.

Today, the mainstream approach is focused on the development of optical systems that offer a narrow band spectral selectivity and multi-color detection, which became a key parameter for the development of new photodiodes. The strategy relies in the modification of either the composition or the thickness of the photoactive layer using narrowband materials for the active layer to tune its optical absorption exclusively to the region of interest where both the donor and acceptor materials absorb only in the desired wavelength range. Deckman *et al.* developed a fully-printed OPD array capable of RGB light separation printed on a PEN substrate by blade-coating PEDOT:PSS, a polyethylenimine cathode interlayer and the photo-active layer, and screen-printing on top a patterned PEDOT:PSS anode, achieving an average EQE of ~37% at -4V bias over the whole visible spectrum, a dark current of 0.5 $nAcm^{-2}$ and five orders of magnitude of LDR. This broadband OPD is an example of a photodiode that can simplify the fabrication of a spectral-selective photosensor and full-color imagers.[31]

Chuang *et al.* also reported an example of an highly sensitive OPD that had an extended spectral response, from the UV to NIR (~1200 nm). Incorporating two NIR dopants into the OPD, the device exhibit simultaneously a broad spectral response (with R= 23 $AW^{-1}$ under a lower reverse bias, -3.5V), and a good quantum efficiency (EQE ~5500%).[35]

Currently, the range of available semiconductors is very high, and OPDs production processes are far appealing due to their simplicity. For example, Strobel *et al.* described the first inkjet and aerosol-jet printed OPD. Exploring the high-performance of non-fullerene acceptor IDTBR combined with P3HT, this digitally printed device exhibit a broadband spectral response with responsivities up to 300 $mAW^{-1}$ that can compete directly with current available technologies based on Si.[32]

If the electrostatic forces are higher in the acceptor than in the donor, then the interfacial electric field drives charge separation, promoting photogenerated excitons break up, thus improving device efficiency. Yet, organic photodiodes are still a challenge, with some flaws that need to be overcome. These include photocurrent sensitivity to temperature, low charge carrier mobility, thickness dependence, limited light absorption across the solar spectrum and also the need of a strong driving force to break up photogenerated excitons.

## HYBRID PHOTODIODES

Although both inorganic and organic photodiodes have shown some disadvantages and drawbacks, precluding higer expansion to the market, when combined they overcome most of these issues, one of the reasons why organic-inorganic hybrid photodiodes (HPDs) have drawn tremendous attention in past few years.

With unique physical properties such as low temperature solution processability, high photosensitivity or mechanical flexibility, combined with the freedom of rational designing of numerous combinations between organic polymeric and inorganic semiconductors, HPDs revolutionized the world of photodiodes with new applications in astronomy, nuclear physics or spectroscopy.[37,38]

The *p-n* junctions of HPDs usually takes advantage of the intrinsic properties of *n*- type of silicon and several III-V and II-VI semiconductors, such as ZnO, ZnSe CdSe nanocrystals, or GaN, that have an higher electron mobility, with the *p*-type nature of organic semiconductors, usually polymeric materials such as PEDOT:PSS, P3HT or graphene, with higher hole mobility, photosensitivity and optical properties than inorganic semiconductors.[37,39-42] Also, inorganic-organic hybrid halide perovskites, combined with different conductive polymers (*e.g.* PDPP3T PCBM, or PEDOT) and inorganic semiconductors (*e.g.* Si, Ga) have aroused much interest, due to their long carrier diffusion length, low excitation binding and bandgap tunability, still air deterioration is an unsolved problem.[43-46]

HPD devices are now more stable, with longer lifetimes, and in some cases working at lower dark currents. However, the strategy to incorporate hybrid materials implies a deeper investigation in the impact of these materials in the device performance. For example, Pickett *et al.* have shown the influence of two diketopyrrolopyrrole (DPP)-based donor-acceptor copolymers with different backbone conformations incorporated in an inverted non-fullerene photodiode architecture. Using ZnO nano-patterned films as the electron transport layer, photoresponsivity is highly affected. This behaviour could be explained with an enhanced transport of carriers, due to the planar backbone conformation of the PBDT-TTDPP copolymer.[39]

One of the biggest challenges of HPDs development is related to low dark current operation. A huge number of combinations between the inorganic and organic is possible, and device fabrication may differ quite significantly. BHJs have been widedly used to fabricate HPDs photoactive layers. Due to the large *p-n* interfacial area, BHJs are able to produce ideal photo-generated charge separation, however, high reverse saturation current related with the charge injection may turn a disadvantage. Nevertheless, there is always the possibility to form a lower electron barrier into

cathode/*n*-semiconductor interface and a lower hole injection barrier between the anode/*p*-semiconductor interface, making the option of using planar heterojunctions also beneficial in some cases. In this sense, HPDs are typically built in a mixed planar heterojunction/BHJ organic semiconductor architecture. Also the production of inverted HPDs, where the polarity of charge collection is inverted (following the positive results obtained for some organic photodiodes),[31] has gained considerable attention, once device stability may be increased along with easier production. Figure 5 shows one example of an inverted HPD architecture.[18,37,39]

Inverted architectures using nanocrystals are also an interesting approach. Ha *et al.* developed a planar heterojunction composed by PBDTT-FTTE and CdSe nanocrystals having a low dark current and a high detectivity, which is an attractive alternative to produce digital image sensors.[37] Dou *et al.* also demonstrated that inverting a halide perovskite HPD device highly improve its performance.

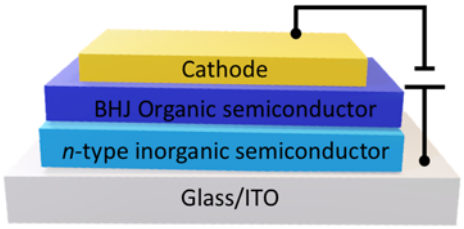


**Figure 5.** Schematic representation of an inverted HPD architecture.

Operating at room temperature, the photodetectors exhibit a large detectivity ($10^{14}$ Jones), a linear dynamic range (over 100 dB) and a fast photoresponse with a 3-dB bandwidth up to 3 MHz.[47]

**Table 1:** Recent examples of photodiodes developed for imaging and X-ray applications.[§]

| Material | Type | Year | D* (Jones) | Responsivity ($AW^{-1}$) | EQE (%) | Application | Ref. |
|---|---|---|---|---|---|---|---|
| **Au-PbS CQD** | Inorganic (Schottky) | 2018 | $1.96\times10^{10}$ | 5.15 | 400 | Optoelectronic circuits and IR focal plane arrays | 26 |
| **n-$Mg_2Si$ single Crystal** | Inorganic (Schottky) | 2019 | - | 0.014[a] | - | Short wavelength IR light | 48 |
| **$Cu(acac)_2$/n-Si** | HPD | 2018 | $4.6\times10^{9}$ | 0.009 | 5.53-8.34 | UV photodetector | 49 |
| **Si/$Bi_2Te_3$-graphene**[b] | HPD | 2019 | $2\times10^{9}$ | 8.9 | 17.4 | Light sensing | 50 |
| **$FAPbBr_3$ QDs/graphene** | HPD | 2018 | - | $1.154\times10^{5}$ | $3.42\times10^{7}$ | Low intensity image sensor | 51 |
| **PEIE/PCDTBT:PC70BM/$MoO_x$** | OPD | 2019 | $10^{3}$ | - | - | Color discrimination | 52 |
| **Perovskite/Black Phosphorus /$MoS_2$** | HPD | 2019 | $1.3\times10^{3}$ | 11 | 80 | Sensor | 53 |
| **PEDOT:PSS/Merocyanine (Pyrl)/$C_{60}$**[c] | OPD | 2019 | - | 0.71 | 18 | Ultranarrowband organic photodiodes | 54 |
| **Lisicon PV-D4650:PCBM**[d] | OPD | 2019 | $2.19\times10^{13}$ | 0.44 | 82 | Image sensors | 55 |
| **$MoO_3$/BHJ/LiF:Al** | OPD | 2019 | | | | | |
| *Red* | | | $1.55\times10^{12}$ | - | 18 | | |
| *Green* | | | $1.89\times10^{12}$ | - | 19.6 | Image sensors | 56 |
| *Blue* | | | $1.8\times10^{12}$ | - | 24.6 | | |
| *Panchromatic* | | | $10.1\times10^{12}$ | - | 65.1 | | |
| **GR/GQDs**[e] | DUV PD | 2019 | $1.1\times10^{13}$ | 0.11 | - | DUV optoelectronic devices | 57 |
| **$(PEA)_2(MA)_{59}Pb_{60}I_{181}$/Spiro-OMeTAD** | HPD | 2019 | $2.2\times10^{12}$ | 0.53 | - | Photodiodes applications | 58 |
| **Si type** | Inorganic | 2019 | - | 0.274 | ~45 | X-ray | 59 |
| **$MoO_x$/DBP/DBP:$C_{60}$/$C_{60}$/BCP** | OPD | 2019 | - | - | ~37 | Optoelectronic pulse meter sensor | 60 |

[§] Measurements performed at particular wavelenghts are specified. [a]1.4 µm. [b]635 nm. [c]481 nm. [d]660 nm. [e]256 nm.

## RECENT ADVANCES

In the last decades, we witnessed a huge evolution in photodiodes, with special focus on the use of improved materials and architectures, that allowed the development of new types of photodiodes for specific applications. Table 1 lists a selection of recent progress that has been made in the field.

Enanched photodiodes (faster, more responsive, with high detectivity and low dark current), have been developed using materials such as nanocrystals,[12,41] quantum dots,[61] halide perovskites,[46,51] ZnSSe-*p*-GaAs,[62] and polymer blends (*e.g.* PCBM and MEHPPV).[63] Image sensing (*e.g.* CMOS active pixel sensors)[16,31,64,65] is one of the most important applications of photodiodes, but other type of image sensors for cell imaging,[66] to be used under cryogenic conditions[67,68] or in space[69] are also emergent challenges.

Photodiodes play an important role in medicine. Simple X-ray detection[70-72] and pulse oxametry are key examples of applications. Pulse oxametry is of major importance in routine clinics since is a efficient and non-invasive way to measure blood oxygen saturation. In this case, the use of flexible materials is an huge advantage, allowing wearable devices (*e.g.* ring-shaped)[73] that can be used in fingers, feet, forehead, chest or wrists.[74-76] In cardiovascular related diseases they are used in monitorization (usually silicon-based avalanche photodiodes),[77,78] in blood volume measurements (photoplethysmograms), in early detection of some cardiovascular problems,[79] or in Positron Emission Tomography–Magnetic Resonance Imaging (PET-MRI).[80] Other bioaplications such as artificial retinal implants,[33] smart for monitoring vital signs,[81] or bio-HPD that contain DNA have been also explored.[82]

Another interesting application is the detection of analytes by fluorescence and chemiluminescence using microfluidic systems.[83,84] Here, the development of organic and hybrid photodiodes was crucial, since the devices use small molecules such as copper phtalocyanine and fluorene or polymers such as PCDTBT, PH3T or $PC_{60}BM$ to fabricate fluorescence detectors for biomarkers and molecular probes, and chemiluminescent sensors.[34,85,86] These microfluidic biosensors allowed the detection of phatogens such as *E. coli* or *Campylobacter jejuni*.[87]

## FINAL REMARKS

In symmary, in the past few years research on photodiodes devices fabrication and optimization reached a tremendous progress. The unique properties of HPDs are fostering the field of optoelectronics and triggering novel applications. Still far from perfection, future work should focus on the exploitation of hybrid systems, taking advantage of the unlimited combinations of organic and inorganic components. Future design should still pursue an *ideal* architecture, combining a good equilibrium between high gain, detectivity, responsivity, EQE, and broad spectral working range.

## ACKNOWLEDGMENTS

We thank Fundação para a Ciência e a Tecnologia (FC&T, Lisbon) for financial support through projects EXPL/CTM-ENE/1502/2013 and PhD grant SFRH/BD/109006/2015 (R.F.P).

## REFERENCES AND NOTES

1. A. Armin, M. Hambsch, I.K. Kim, P.L. Burn, P. Meredith, E.B. Namdas. Thick junction broadband organic photodiodes. *Laser Photonics Rev.* **2014**, 8(6), 924–932.
2. X. Liu, Y. Lin, Y. Liao, J. Wu, Y. Zheng. Recent advances in organic near-infrared photodiodes. *J. Mater. Chem. C* **2018**, 6(14), 3499–3513.
3. P.S. Bui, N.D. Taneja, U.S. Patent 6 593 636 B1, **2003**.
4. R.A. Schmidt, M.O. Perley, R.A. Kuehm, U.S. Patent 8 290 726 B2, **2012**.
5. D. Yang, D. Ma. Development of organic semiconductor photodetectors: From mechanism to applications. *Adv. Optical Mater.* **2018**, 7(1), 1800522.
6. G. Ripoche, J. Harari. Optoelectronic sensors, John Wiley & Sons: Hoboken, **2009**.
7. B. Gray, Wiley Encyclopedia of Biomedical Engineering, John Wiley & Sons: Portsmouth, **2006**.
8. D. Renker. Geiger-mode avalanche photodiodes, history, properties and problems. *Nucl. Instrum. Methods Phys. Res. A* **2006**, 567(1), 48–56.
9. A. Reznik, W. Zhao, Y. Ohkawa, K. Tanioka, J.A. Rowlands. Applications of avalanche multiplication in amourphous selenium to flat panel detectors for medical applications. *J. Mater. Sci: Mater. Electron.* **2009**, 20(S1), 63–67.
10. O. Hayden, R. Agarwal, C.M. Lieber. Nanoscale avalanche photodiodes for highly sensitive and spatially resolved photon detection. *Nat. Mater.* **2006**, 5(5), 352–356.
11. Z. Alaie, S.M. Nejad, M.H. Yousefi. Recent advances in ultraviolet photodetectors. *Mater. Sci. Semicond. Process.* **2015**, 29, 16–55.
12. M. Baibarac, P. Gómez-Romero. Nanocomposites based on conducting polymers and carbon nanotubes: From fancy materials to functional applications. *J. Nanosci. Nanotechnol.* **2006**, 6(2), 289–302.
13. R. Saran, R.J. Curry. Lead sulphide nanocrystal photodetector technologies. *Nat. Photonics* **2016**, 10(1), 81–92.
14. S. Riazimehr, S. Kataria, R. Bornemann, P.H. Bolívar, F.J.G. Ruiz, O. Engström, A. Godoy, M.C. Lemme. High photocurrent in gated graphene-silicon hybrid photodiodes. *ACS Photonics* **2017**, 4(6), 1506–1514.
15. F. Bouzid, L. Dehimi, F. Pezzimenti. Performance analysis of a Pt/n-GaN schottky barrier UV detector. *J. Electron. Mater.,* **2017**, 46(11), 6563-6570.
16. R.D.J. Vuuren, A. Armin, A.K. Pandeley, P.L. Burn, P. Meredith. Organic photodiodes: The future of full color detection and image sensing. *Adv. Mater.* **2016**, 28 (24), 4766–4802.
17. R.J. Keyes, P.W. Kruse, D. Long, A.F. Milton, E.H. Putley, M.C. Teich, H.R. Zwicker. Optical and infrared detectors *in* Topics in applied physics, Vol. 19 (R. J. Keyes Ed.), Springer-Verlag, Berlin, **1977**.
18. L. Shi, Q. Liang, W. Wang, Y. Zhang, G. Li, T. Ji, Y. Hao, Y. Cui. Research progress in organic photomultiplication photodetectors. *Nanomaterials* **2018**, 8(9), 713.
19. S. Arikata, T. Kyono, K. Miura, S. Balasekaran, H. Inada, Y. Iguchi, M. Sakai, H. Katayama, M. Kimata, K. Akita. Structural and electrical properties of InAs/GaSb superlattices grown by metalorganic vapor phase epitaxy for midwavelength infrared detectors. *Phys. Status Solidi A* **2017**, 214(3), 1600582.
20. Y. Qin, S. Long, H. Dong, Q. He, G. Jian, Y. Zhang, X. Hou, P. Tan, Z. Zhang, H. Lv, Q. Liu, M. Liu. Review of deep ultraviolet photodetector based on gallium oxide. *Chin. Phys. B* **2019**, 28(1), 018501.
21. N. Huo, G. Konstantatos. Recent progress and future prospects of 2D-based photodetectors. *Adv. Mater.* **2018**, 30(51), 1801164.
22. X. Liu, G. Sun, P. Chen, J. Liu, Z. Zhang, J. Li, H. Ma, B. Zhao, R. Wu, W. Dang, X. Yang, C. Dai, X. Tang, Z. Chen, L. Miao, X. Liu, B. Li, Y. Liu, X. Duan. High-performance asymmetric electrodes photodiode based on Sb/WSe2 heterostructure. *Nano Res.* **2019**, 12(2), 339–344.
23. G.M. Kumar, F. Xiao, P. Ilanchezhiyan, Sh. Yuldashev, A.M. Kumar, H.D. Cho, D.J. Lee, T.W. Kang. High performance photodiodes based on chemically processed Cu doped $SnS_2$ nanoflakes. *Appl. Surf. Sci.* **2018**, 455, 446–454.
24. J. Liu, Y. Li, Y. Song, Y. Ma, Q. Chen, Z. Zhu, P. Lu, S. Wang. $Bi_2Te_3$ photoconductive detectors on Si. *Appl. Phys. Lett.* **2017**, 110(14), 141109.
25. P. Wangyang, C. Gong, G. Rao, K. Hu, X. Wang, C. Yan, L. Dai, C. Wu, J. Xiong. Recent advances in halide perovskite photodetectors based on different dimensional materials. *Adv. Optical Mater.* **2018**, 6(11), 1701302.

26. Y. Tang, F. Wu, F. Chen, Y. Zhou, P. Wang, M. Long, W. Zhou, Z. Ning, J. He, F. Gong, Z. Zhu, S. Qin, W. Hu. A colloidal-quantum-dot infrared photodiode with high photoconductive gain. *Small* **2018**, 14(48), 1803158.
27. S. Siontas, H. Wang, D. Li, A. Zaslavsky, D. Pacifici. Broadband visible-to-telecom wavelength germanium quantum dot photodetectors. *Appl. Phys. Lett*. **2018**, 113(18), 181101.
28. X. Gong, M. Tong, Y. Xia, W. Cai, J.S. Moon, Y. Cao, G. Yu, C.-L. Shieh, B. Nilsson, A.J. Heeger. High-detectivity polymer photodetectors with spectral response from 300 nm to 1450 nm. *Science* **2009**, 325(5948), 1665–1667.
29. T. Dhawan, Aarti, A. Kotnala, B.S. Chhikara. Organic Light Emitting Diode: Energy efficient material for sustainable green environment, *Proceedings of National Conference RACSGSE-SBAP*, **2017**, 45-56.
30. S. Yoon, K. Min. Sim, D.S. Chung. Prospects of colour selective organic photodiodes. *J. Mater. Chem. C* **2018**, 6(48), 13084–13100.
31. I. Deckman, P.B. Lechêne, A. Pierre, A.C. Arias. All-printed full-color pixel organic photodiode array with a single active layer. *Org. Electron.* **2018**, 56, 139–145.
32. N. Strobel, M. Seiberlich, T. Rödlmeier, U. Lemmer, G. Hernandez-Sosa. Non-fullerene based printed organic photodiodes with high responsivity and MHz detection speed. *ACS Appl. Mater. Interfaces* **2018**, 10(49) 42733–42739.
33. G. Simone, D.D.C. Rasi, X. de Vries, G.H.L. Heintges, S.C.J. Meskers, R.A.J. Janssen, G.H. Gelinck. Near-infrared tandem organic photodiodes for future application in artificial retinal implants. *Adv. Mater.* **2018**, 30(51), 1804678.
34. J.R. Wojciechowski, L.C. Shriver-Lake, M.Y. Yamaguchi, E. Füreder, R. Pieler, M. Schamesberger, C. Winder, H.J. Prall, M. Sonnleitner, F.S. Ligler. Organic photodiodes for biosensor miniaturization. *Anal. Chem.* **2009**, 81(9), 3455–3461.
35. S.-T. Chuang, S.-C. Chien, F.-C. Chen. Extended spectral response in organic photomultiple photodetectors using multiple near-infrared dopants. *Appl. Phys. Lett.* **2012**, 100(1), 013309.
36. R. Zhao, U. S. Patent 2019/0013360A1, **2019**.
37. J. Ha, S. Yoon, J.-S. Lee, D.S. Chung. Organic-inorganic hybrid inverted photodiode with planar heterojunction for achieving low dark current and high detectivity. *Nanotechnology* **2016**, 27(9), 095203.
38. J. Singh, R.G. Singh, S.K. Gautam, F. Singh. Multifunctional hybrid diode: Study of phosphorescence, high responsivity, and charge injection mechanisms. *J. Appl. Phys.* **2018**, 123(17), 174503.
39. A. Pickett, A. Mohapatra, A. Laudari, S. Khanra, T. Ram, S. Patil, S. Guha. Hybrid ZnO-organic semiconductor interfaces in photodetectors: A comparison of two near-infrared donor-acceptor copolymers. *Org. Electron.* **2017**, 45, 115–123.
40. A.D. Bartolomeo, G. Luongo, F. Giubileo, N. Funicello, G. Niu, T. Schroeder, M. Lisker, G. Lupina. Hybrid graphene/silicon Sckottky photodiode with intrinsic gating effect. *2D Mater.* **2017**, 4(2), 025075.
41. J.-J. Wang, Y.-Q. Wang, F.-F. Cao, Y.-G. Guo, L.-J. Wan. Synthesis of monodispersed wurtzite structure $CuInSe_2$ nanocrystals and their application in high-performance organic-inorganic hybrid photodetectors. *J. Am. Chem. Soc.* **2010**, 132(35), 12218–12221.
42. S.S. Mousavi, B. Sajad, M.H. Majlesara. Fast response ZnO/PVA nanocomposite-based photodiodes modified by graphene quantum dots. *Mater. Des.* **2019**, 162, 249–255.
43. F. Zhao, K. Xu, X. Luo, Y. Liang, Y. Peng, F. Lu. Toward high uniformity of photoresponse broadband hybrid organic-inorganic photodiode based on PVP-modified perovskite. *Adv. Optical Mater.* **2018**, 6(1), 1700509.
44. X. Liu, D. Yu, F. Cao, X. Li, J. Ji, J. Chen, X. Song, H. Zeng. Low-voltage photodetectors with high responsivity based on solution-processed micrometer-scale all-inorganic perovskite nanoplatelets. *Small* **2017**, 13(25), 1700364.
45. Y. Wang, D. Yang, X. Zhou, D. Ma, A. Vadim, T. Ahamad, S.M. Alshehri. Perovskite/polymer hybrid thin films for high external quantum efficiency photodetectors with wide spectral response from visible to near-infrared wavelengths. *Adv. Optical Mater.* **2017**, 5(12), 1700213.
46. F. Zhao, K. Xu, X. Luo, W. Lv, Y. Peng, Y. Wang, F. Lu, S. Xu. Ultrasensitivity broadband photodetectors based on perovskite: Research on film crystallization and electrode optimization. *Org. Electron.* **2017**, 46, 35–43.
47. L. Dou, Y. Yang, J. You, Z. Hong, W.-H. Chang, G. Li, Y. Yang, Solution-processed hybrid perovskite photodetectors with high detectivity. *Nat. Commun.* **2014**, 5, 5404.
48. A.A.M. El-Amir, T. Ohsawa, T. Nabatame, A. Ohi, Y. Wada, M. Nakamura, X. Fu, K. Shimamura, N. Ohashi. Ecofriendly $Mg_2Si$-based photodiode for short-wavelength IR sensing. *Mater. Sci. Semicond. Process.* **2019**, 91, 222–229.
49. H. Abdel-Khalek, M.I. El-Samahi, M.A.-El Salam, A.M. El-Mahalawy, Fabrication and performance evaluation of ultraviolet photodetector based on organic /inorganic heterojunction. *Curr. Appl. Phys.***2018**, 18(12), 1496–1506.
50. A. Parbatani, E.S. Song, J. Claypoole, B. Yu. High performance broadband bismuth telluride tetradymite topological insulator photodiode. *Nanotechnol.* **2019**, 30, 165201.
51. R. Pan, H. Li, J. Wang, X. Jin, Q. Li, Z. Wu, J. Gou, Y. Jiang, Y. Song. High-responsivity photodetectors based on formamidinium lead halide perovskite quantum dot–graphene hybrid. *Part. Part. Syst. Charact.* **2018**, 35 (4), 1700304.
52. A. Yazmaciyan, P. Meredith, A. Armin. Cavity enhanced organic photodiodes with charge collection narrowing. *Adv. Optical Mater.* **2019**, 7(8), 1801543.
53. L. Wang, X. Zou, J. Lin, J. Jiang, Y. Liu, X. Liu, X. Zhao, Y.F. Liu, J.C. Ho, L. Liao. Perovskite/black phosphorus/$MoS_2$ photogate reversed photodiodes with ultrahigh light on/off ratio and fast response. *ACS Nano* **2019**, 13 (4), 4804–4813.
54. A. Liess, A. Arjona-Esteban, A. Kudzus, J. Albert, A.-M. Krause, A. Lv, M. Stolte, K. Meerholz, F. Würthner. Ultranarrow bandwidth organic photodiodes by exchange narrowing in merocyanine H- and J-aggregate excitonic systems. *Adv. Funct. Mater.* **2019**, 29 (21), 1805058.
55. M. Biele, C.M. Benavides, J. Hürdler, S.F. Tedde, C.J. Brabec, O. Schmidt. Spray-coated organic photodetectors and image sensors with silicon-like performance. *Adv. Mater. Technol.* **2019**, 4 (1), 1800158.
56. S. Yoon, K.M. Sim, D.S. Chung. Bifunctional etalon-electrode to realize high-performance color filter free image sensor. *ACS Nano* **2019**, 13 (2), 2127–2135.
57. C.W. Jang, D.H. Shin, S.-H. Choi, Highly-flexible and -stable deep-ultraviolet photodiodes made of graphene quantum dots sandwiched between graphene layers. *Dyes Pigm.* **2019**, 163, 238–242.
58. J.W. Lima, H. Wanga, C.H. Choia, H. Kwona, L.N. Quand, W.-T. Parke, Y.-Y. Nohe, D.H. Kima. Self-powered reduced-dimensionality perovskite photodiodes with controlled crystalline phase and improved stability. *Nano Energy* **2019**, 57, 761–770.
59. Q. Looker, B.A. Aguirre, M.E. Hoenk, A.D. Jewell, M.O. Sanchez, B.D. Tierney. Superlattice-enhanced silicon soft X-ray and charged particle detectors with nanosecond time response. *Nucl. Instrum. Methods Phys. Res. Sect. A* **2019**, 916, 148–153.
60. F. Elsamna, A. Bilgaiyan, M. Affiq, C.-H. Shim, H. Ishidai, R. Hattori. Comparative design study for power reduction in organic optoelectronic pulse meter sensor. *Biosensors* **2019**, 9(2), 48.
61. T. Rauch, M. Böberl, S.F. Tedde, J. Fürst, M.V. Kovalenko, G. Hesser, U. Lemmer, W. Heiss, O. Hayden. Near-infrared imaging with quantum-dot-sensitized organic photodiodes. *Nat. Photonics* **2009**, 3, 332–336.
62. T. Abe, D. Katada, K. Miki, K. Tanaka, M. Nomura, Y. Inagaki, T. Tani, M. Ohtsuki, H. Kasada, K. Ando. High sensitive ultravioleta organic- inorganic hybrid photodetectors on ZnSSe grown on p-GaAs with transparent conducting polymer window-layer. *Phys. Status Solidi C* **2010**, 7(6), 1706–1708.
63. T.N. Ng, W.S. Wong, M.L. Chabinyc, S. Sambandan, R.A. Street. Flexible Image sensor array with bulk heterojunction organic photodiodes. *Appl. Phys. Lett.* **2008**, 92(21), 213303.
64. E.R. Fossum. CMOS image sensors: Electronic camera-on-chip. *IEEE Trans. Electron Devices* **1997**, 44(10), 1689–1698.
65. H. Shekhar, V. Lami, O. Solomeshch, A. Fenigstein, L. Tomer, L. Becky, Y. Vanzof, N. Tessler. Doping induced performance enhancement in inverted small molecule organic photodiodes operating below 1V reverse

bias – Towards compatibility with CMOS for imaging applications. *Org. Electron.* **2019**, 67, 1–9.
66. I. Britvich, I. Johnson, D. Renker, A. Stoykov, E. Lorenz. Characterisation of Geiger-mode avalanche photodiodes for medical imaging applications. *Nucl. Instrum. Methods Phys. Res., Sect. A* **2007**, 571(1-2), 308–311.
67. X. Tang, M.M. Ackerman, M. Chen, P. Guyot-Sionnest. Dual-band infrared imaging using stacked colloidal quantum dot photodiodes. *Nat. Photonics* **2019**, 13, 277–282.
68. B.L. Glebov, A. Waczynski, K.S. Jepsen, L.R. Miko. Stability of device responsivity in silicon photodiodes under cryogenic conditions. *Rev. Sci. Instrum.* **2018**, 89(11), 113106.
69. W.-T. Kim, C. Park, H. Lee, I. Lee, B.-G. Lee. A high full well capacity CMOS image sensor for space applications. *Sensors* **2019**, 19(7), 1505.
70. T. Agostinelli, M. Campoy- Quiles, J.C. Blakesley, R. Speller, D.D.C. Bradley, J. Nelson. A polymer/fullerene based photodetector with extremely low dark current for x-ray medical imaging applications. *Appl. Phys. Lett.* **2008**, 93(20), 203305.
71. B.-C. Juang, A. Chen, D. Ren, B. Liang, D.L. Prout, A.F. Chatziioannou, D.L. Huffaker. Energy-sensitive GaSb/AlAsSb separate absorption and multiplication avalanche photodiodes for x-ray and gamma-ray detection. *Adv. Optical Mater.* **2019**, 1900107.
72. C. Dydula, G. Belev, P.C. Johns. Development and assessment of a multi-beam continuous-phantom-motion x-ray scatter projection imaging system. *Rev. Sci. Instrum.* **2019**, 90, 035104.
73. S.B. Duun, R.G. Haahr, K. Birkelund, E.V. Thomsen. A ring-shaped photodiode designed for use in a reflectance pulse oximetry sensor in wireless health monitoring applications. *IEEE Sens. J.* **2010**, 10(2), 261–268.
74. C.M. Lochner. Y. Khan, A. Pierre, A.C. Arias. All-organic optoelectronic sensor for pulse oximetry. *Nat. Commun.* **2014**, 5, 5745.
75. T. Kaya, G. Liu, J. Ho, K. Yelamarthi, K. Miller, J. Edwards, A. Stannard. Wearable sweat sensors: background and current trends. *Electroanalysis* **2019**, 31(3), 411–442.
76. Y. Yang, W. Gao. Wearable and flexible electronics for continuous molecular monitoring. *Chem. Soc. Rev.* **2019**, 48 (6), 1465–1491.
77. N. Piazza, R.J. Wessells. Drosophila models of cardiac disease. *Prog. Mol. Biol. Transl. Sci.* **2011**, 10, 155–210.
78. T. Pereira, T. Oliveira, M. Cabeleira, H. Pereira, V. Almeida, J. Cardoso, C. Correia. Comparison of low-cost and noninvasive optical sensors for cardiovascular monitoring. *IEEE Sens. J.* **2013**, 13(5), 1434–1441.
79. D.R. Uguz, B. Venema, S. Leonhardt, D. Teichmann. Multifunctional photoplethysmography sensor design for respiratory and cardiovascular diagnosis. *IFMBE Proceedings* **2018**, 68(2), 905–909.
80. G. Arora, N. Damle. Radiopharmaceuticals for diagnosis of Primary Hyperparathyroidism. *Chem. Biol. Lett.*, **2018**, 5(1), 35-40.
81. A. Satharasinghe, T. Hughes-Riley, T. Dias. Photodiodes embedded within electronic textiles. *Sci. Rep.* **2018**, 8, 16205.
82. M.S.P. Reddy, P.T. Puneetha, Y.-W. Lee, S.-H. Jeong, C. Park. DNA-CTMA/a-Si:H bio-hybrid photodiode: A light-sensitive photosensor. *Org. Electron.* **2017**, 50, 435–442.
83. M. Miyake, H. Nakajima, A. Hemmi, M. Yahiro, C. Adachi, N. Soh, R. Ishimatsu, K. Nakano, K. Uchiyama, T. Imato. Performance of an organic photodiode as an optical detector and its application to fluorometric flow-immunoassay for IgA. *Talanta* **2012**, 96, 132–139.
84. I.F. Pinto, D.R. Santos, C.R.F. Caneira, R.R.G. Soares, A.M. Azevedo, V. Chu, J.P. Conde. Optical biosensing in microfluidics using nanoporous microbeads and amorphous silicon thin-film photodiodes: Quantitative analysis of molecular recognition and signal transduction. *J. Micromech. Microeng.* **2018**, 28, 094004.
85. X. Wang, M. Amatatongchai, D. Nacapricha, O. Hofmann, J.C. deMello, D.D.C. Bradley, A.J. deMello. Thin-film organic photodiodes for integrated on-chip chemiluminescence detection-application to antioxidant capacity screening. *Sens. Actuators B Chem.* **2009**, 140(2), 643–648.
86. A. Nascetti, M. Mirasoli, E. Marchegiani, M. Zangheri, F. Costantini, A. Porchetta, L. Iannascoli, N. Lovecchio, D. Caputo, G. Cesare, S. Pirrotta, A. Roda. Integrated chemiluminescence-based lab-on-chip for detection of life markers in extraterrestrial environments. *Biosens. Bioelectron.* **2019**, 123, 195–203.
87. N.M.M. Pires, T. Dong. Microfluidic biosensor array with integrated poly(2,7-carbazole)/fullerene-based photodiodes for rapid multiplex detection of pathogens. *Sensors* **2013**, 13(12), 15898–15911.

## AUTHORS BIOGRAPHIES

**Rita F. Pires** is currently an MIT Portugal PhD candidate at IBB – Institute for Bioengineering and Biosciences, Instituto Superior Técnico, University of Lisbon. Her research is focused in synthesis of dendrimer-based solar supercapacitors. She obtained her BSc degree in 2013 in Applied Chemistry – Organic Chemistry major and finished her MSc in Bioorganic Chemistry in 2015 at NOVA University of Lisbon.

**Vasco D.B. Bonifácio** received his PhD in Chemistry (Organic Chemistry) in 2006. After a post-doc in Scherf's group (Wuppertal, Germany) he was appointed Assistant Researcher of the MIT Portugal Program in 2008. In 2012 he was a visiting researcher at MIT (Boston, USA) in the Hammond's Lab. Currently is a Researcher at IBB – Institute for Bioengineering and Biosciences, Instituto Superior Técnico, University of Lisbon. His main interests are in the fields of Nanomedicine and Molecular Electronics. Currently, his research is focused on the green synthesis (mechanochemistry, sonochemistry and catalyst-free in-water reactions) of complex 3D polymer architectures for Cancer Theranostics and Regenerative Nanomedicine.